Journal of Power Sources 270 (2014) 576–586

Contents lists available at ScienceDirect

Journal of Power Sources

journal homepage: www.elsevier.com/locate/jpowsour

Extended dynamic model for ion diffusion in all-vanadium redox flow battery including the effects of temperature and bulk electrolyte transfer

Rajagopalan Badrinarayanan [a], Jiyun Zhao [a, *], K.J. Tseng [a], Maria Skyllas-Kazacos [b]

[a] EXQUISITUS, Centre for E-City, School of Electrical & Electronic Engineering, Nanyang Technological University, Singapore 639798, Singapore
[b] School of Chemical Engineering, The University of New South Wales, UNSW, Sydney, NSW 2052, Australia

HIGHLIGHTS

- An extended dynamic ion-diffusion model is developed to study capacity loss.
- The temperature effect and bulk electrolyte transfer effect is modeled.
- The established model is benchmarked with experiments.
- The effect of temperature on three different membranes is analyzed.
- Concentration change for individual ions leading to capacity decay was studied.

ARTICLE INFO

Article history:
Received 10 June 2014
Received in revised form
18 July 2014
Accepted 20 July 2014
Available online 1 August 2014

Keywords:
Energy storage
Vanadium redox flow battery
Capacity loss model
Temperature dependence
Bulk electrolyte transfer
Battery efficiency

ABSTRACT

As with all redox flow batteries, the Vanadium Redox flow Battery (VRB) can suffer from capacity loss as the vanadium ions diffuse at different rates leading to a build-up on one half-cell and dilution on the other. In this paper an extended dynamic model of the vanadium ion transfer is developed including the effect of temperature and bulk electrolyte transfer. The model is used to simulate capacity decay for a range of different ion exchange membranes that are being used in the VRB. The simulations show that Selemion CMV and Nafion 115 membranes have similar behavior where the impact of temperature on capacity loss is highest within the first 100 cycles. The results for Selemion AMV membrane however are seen to be very different where the capacity loss at different temperatures observed to increase linearly with increasing charging/discharging cycles. The model is made more comprehensive by including the effect of bulk electrolyte transfer. A volume change of 19% is observed in each half-cell for Nafion 115 membrane based on the simulation parameters. The effect of this change in volume directly affects concentration, and the characteristics are analyzed for each vanadium species as well as the overall concentration in the half-cells.

1. Introduction

Redox flow cell energy storage systems are becoming increasingly popular because of the numerous advantages they offer. These systems are modular, highly efficient and the cost is relatively low which makes it easy to scale up [1,2]. Another advantage of redox flow batteries is that the power and energy aspects of a battery are decoupled which makes it very convenient and efficient to design the battery configurations for applications such as load leveling, area and frequency regulation, grid integration and peak shaving [1–5].

One of main reasons that the Vanadium Redox battery is popular among the redox flow batteries is due to the fact that both the half cells of the battery employ different species of vanadium in the electrolyte [3,6]. As a result, the problem of cross contamination during long term usage is eliminated and the lifetime of the electrolyte is significantly extended [3,7]. Also, it was found that the environmental impact caused by the VRB is lower in comparison to other conventional ones like the lead acid battery [8].

* Corresponding author. Tel.: +65 6790 4508; fax: +65 6793 3318.
E-mail address: jyzhao@ntu.edu.sg (J. Zhao).

http://dx.doi.org/10.1016/j.jpowsour.2014.07.128
0378-7753/

Nomenclature

c_2	concentration of V^{2+} ions (mol L^{-1})
c_3	concentration of V^{3+} ions (mol L^{-1})
c_4	concentration of V^{4+} ions (mol L^{-1})
c_5	concentration of V^{5+} ions (mol L^{-1})
c_{H^+}	concentration of H^+ ions (mol L^{-1})
c_{H^+}neg	concentration of H^+ ions in the negative half-cell (mol L^{-1})
c_{H^+}pos	concentration of H^+ ions in the positive half-cell(mol L^{-1})
D_2	maximum diffusion coefficient of V^{2+} ions (dm^2 s^{-1})
D_3	maximum diffusion coefficient of V^{3+} ions (dm^2 s^{-1})
D_4	maximum diffusion coefficient of V^{4+} ions (dm^2 s^{-1})
D_5	maximum diffusion coefficient of V^{5+} ions (dm^2 s^{-1})
D_{H^+}	diffusion coefficient of H^+ ions (dm^2 s^{-1})
J	current density (A cm^{-2})
E_a	activation Energy (J mol^{-1})
S_M	membrane surface area (dm^2)
S_E	electrode surface area (cm^2)
V	electrolyte volume (dm^3)
R	universal gas constant (J K^{-1} mol^{-1})
T	temperature (K)
z	number of electrons transferred in the reaction
F	Faraday's constant (C mol^{-1})
d	thickness of membrane (dm)
E'_0	formal potential (V)
SOC	state of charge
ΔV	change in volume after each cycle (L)
$\overrightarrow{v}_m$	velocity term for electrolyte across the membrane (m s^{-1})
Δt	time taken for one iteration (sec)
k_p	hydraulic permeability (m^2)
k_ϕ	electro kinetic permeability (m^2)
c_f	fixed acid concentration (mol m^{-3})
C_{norm}	normalized concentration term
V_n	volume of negative half-cell (L)
V_p	volume of positive half-cell (L)
i_{tot}	charging/discharging stack current (A)
R_m	electrical resistance of the membrane (Ω)
r_m	local resistivity of the membrane (Ω m^{-2})

Greek symbol

$\Delta\Pi_{osmotic}$	change in pressure difference between half-cells (Pa)
φ_m	ionic potential (V)

Subscript

2	V^{2+} ions
3	V^{3+} ions
4	V^{4+} ions
5	V^{5+} ions
H^+	hydrogen ions
M	membrane
E	electrode
(charging)	during charging process
(discharging)	during discharging process
tot	total

A Vanadium Redox Battery has vanadium ions reacting in both half cells of the battery, each being separated by an ion exchange membrane which allows H^+ ions to pass through to maintain charge balance. An ideal ion exchange membrane should limit the flow of vanadium ions through it and should possess good conductivity and chemical stability [9]. A lot of research has gone into improving this very important part of the battery which is very vital for maintaining the capacity of the battery during long term cycling [10–13]. No membrane is 100% selective however, so vanadium ions are still able to diffuse through the membrane from one half-cell to the other. The differential rate of vanadium ion diffusion across the membrane is one of the major causes of capacity loss when there is an accumulation of vanadium in one half-cell and a decrease in the other. Although the self-discharge reactions between the vanadium ions across the membrane lead to capacity fade, this can be readily restored by simply remixing the two half-cell solutions periodically [14]. On the other hand, other side reactions such as air oxidation of V^{2+} and the evolution of hydrogen in the negative electrolyte and the electrode respectively also result in capacity loss, but this cannot be restored by simple remixing of the electrolytes and requires a chemical or electrochemical rebalance [7,14]. Several approaches have been proposed to reduce capacity fade by varying the operating conditions of the battery [15,16].

The type of the membrane used determines the rates of water transfer and vanadium ion diffusion across the membrane, which in turn affects both capacity fade and coulombic efficiency [17]. Extensive research has been carried out for improvement of the membrane to minimize the water and electrolyte transfer which in turn reduces operational problems and capacity loss in the battery [9,15–17]. Furthermore, a sophisticated SOC monitoring and control system is very important in managing the electrolytes and maintaining balanced half-cells electrolytes [14,18,19] so as to prevent capacity decay in the battery. Before trying to develop a control system, the process of capacity decay needs to be understood in detail.

Over the years, many models have been developed for VRB by researchers all over the world to study the performance of VRB [7,20,21]. A model based on the principles of conservation linked to the kinetics of the reaction is used to simulate the performance of VRB with response to variation of battery parameters was developed by Shah and co-workers [22]. Models focusing particularly on vanadium ion diffusion across the membrane have been reported by Skyllas Kazacos and Goh [23]. Skyllas Kazacos and co-workers developed a dynamic model to study the effects of ion diffusion across the membrane and side reactions on capacity loss in a VRB [7]. They concentrated on simulating capacity loss for different membranes with different rates of hydrogen evolution and V(II) air oxidation during long term charge–discharge cycling operation. More importantly, the ion diffusion rate is dependent on temperature and the temperature stability is different for different species of vanadium ions [24,25]. Tang et al. [26] developed a model that predicts electrolyte temperature and capacity loss in a VRB employing a Nafion 115 membrane. In this model, the Arrhenius equation is used to model the temperature dependence on the vanadium ion diffusion coefficients for Nafion 115. A range of different membranes can be employed in the VRB however, so it would be useful to extend this temperature depended model further to evaluate the capacity decay caused by ion diffusion for a range of different membranes and individually study the effect on different vanadium ion species.

The present model further includes the effect of bulk electrolyte transfer across the membrane which occurs during battery operation and results in a change of volume in each half cell. Even though

the overall volume of the battery remains constant; the difference in volume in each half cell has considerable effect on the battery capacity and performance. Earlier models in the same domain focused more on an overall study of the phenomena and also on very specific parameters that contribute to the electrolyte transfer. This paper aims at extending earlier models that investigate the effect of temperature and bulk electrolyte transfer on diffusion across membrane and provide a comprehensive model to analyze the effect of bulk transfer and temperature on changes in concentration of each vanadium ion species.

2. The effect of temperature on the diffusion rates

A temperature dependent model was developed by Tang et al. [26] that used the Arrhenius Equation to predict the effect of temperature on the diffusion coefficients of the vanadium ions across a Nafion 115 membrane. The Arrhenius model denoting the temperature dependence of diffusion coefficient is given by (1).

$$k_i = D_i e^{-E_A/(RT)} \tag{1}$$

where k_i is the diffusion coefficient, D_i is the maximum diffusion coefficient (when temperature tends to infinite), i denote the vanadium ion species, E_A is the activation energy, T is the temperature in kelvins and R is the gas constant. The activation energy is taken as 17,341 J mol^{-1} assuming that the activation energy is same for each of the vanadium ion species [26]. Further, D_o for each species is calculated by considering the values of diffusion coefficient under standard temperature [7]. The relationship between the diffusion coefficient and temperature at different temperatures for Selemion CMV, Selemion AMV and Nafion 115 membranes is shown in Fig. 1.

3. Model development

The temperature of the battery is an important factor in defining its performance and capacity decay during long term operation. Stack and electrolyte temperature are influenced by many factors such as atmospheric temperature, electrolyte flow rate, heat generated from stack resistance losses and self-discharge reactions as well as the rate of heat transfer through the pipes and stack. The dramatic effects of the self-discharge reactions on stack temperature, especially in idle mode when the pumps are switched off, were highlighted in the thermal model and simulations by Tang et al. [26]. The importance of pump control was discussed as a means of preventing excessive heat generation that could lead to stack deterioration and thermal precipitation of V(V) ions within the stack. The vanadium ions used in the battery precipitate at different temperatures and this can also result in capacity loss. For example, the precipitation of V(II) and V(III) ions happen in the negative half-cell electrolyte when the temperatures drops, typically below 5 °C, depending on electrolyte composition. On the other hand, V(V) ions in the positive electrolyte tend to precipitate at elevated temperatures. This could lead to blocking of electrolyte channels and result in a deterioration in the capacity and performance of the battery [26–28]. A model that can accurately predict the concentrations of each of the vanadium species in the two half-cells will help in the development of an electrolyte management system that can avoid potential precipitation problems during long-term operation of the VRB under different climatic and operating conditions.

In the present study, the proposed addition of bulk electrolyte transfer across the membrane is modeled based on the earlier work in the same domain [22,29–31]. As the electrolyte moves from one half-cell to the other, the loss of electrolyte volume on one side is approximately equal to the increase in electrolyte volume of the other half cell. Slight variations will arise due to non-ideal mixing and variations in electrolyte density [17], however for simplicity, this is neglected here. The change in electrolyte volume for this model is taken at the precision of 500 ms which incorporates even the minor changes providing improved accuracy.

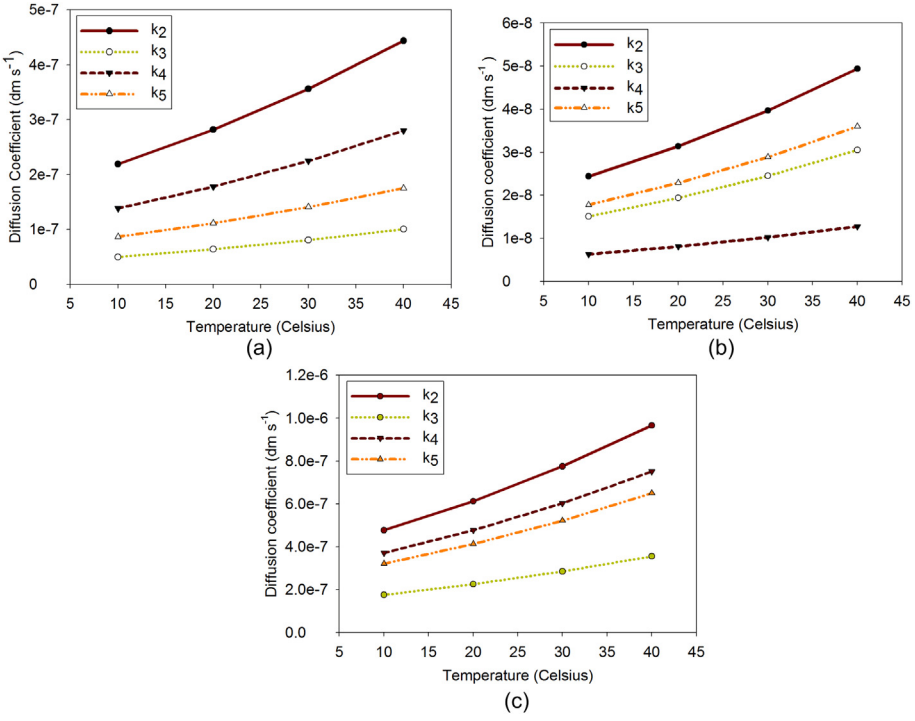

Fig. 1. Diffusion coefficients at different temperatures (a) Selemion CMV (b) Selemion AMV (c) Nafion 115.

The small change in electrolyte volume is given by.

$$\Delta V = \vec{v}^{m} S_M \Delta t \tag{2}$$

where $\vec{v}^{m}$ is the velocity of electrolyte across the membrane, S_M is the membrane area and Δt is the time taken for one cycle of operation. The velocity of electrolyte transfer across membrane for any cycle can be given by the alternate form of Schlogl's equation which describes the convective transport of bulk electrolyte [29].

$$\vec{v}^{m} = -\frac{k_p}{\mu_w}\left|\Delta \Pi_{\text{osmotic}}\right| - \frac{k_\varphi}{\mu_w} c_f F \left(\varphi_m - \frac{RT}{F} C_{\text{norm}} - \frac{RT}{F}\left(\frac{D^m_{H^+}\Delta c_{H^+}}{c_{H^+}}\right)\right) \tag{3}$$

This equation accounts for the bulk electrolyte movement due to osmosis, the transfer due to the interactions between the vanadium ions and the fluid and also the water transfer due to the movement of H^+ ions across the membrane. The pressure difference across the half-cells ($\Delta\Pi_{\text{osmotic}}$) can be approximated from the Van't Hoff equation, given by:

$$\Delta \Pi_{\text{osmotic}} = \left[\left((c_2 + c_3) - (c_4 + c_5)\right) + \left(c_{H^+ neg} - c_{H^+ pos}\right)\right] * R * T \tag{4}$$

The equation for osmotic pressure accounts for the pressure difference due to the concentration of vanadium ions at different oxidation states as well as the proton concentration. The proton concentration however does not build up for an ideal proton exchange membrane as there is free movement of proton across the membrane. The issue of proton concentration gradient however might become an issue in the case of prolonged operation of the VRB causing active sites of the membrane being blocked by the larger vanadium ions and also due to rapid charge/discharge causing imbalance in proton concentration.

The volume in the negative half-cell is denoted by V_n and the volume in the positive half-cell is denoted by V_p. The second term of the velocity equation attributes to the drag of fluid molecules along with the vanadium ions during diffusion process and the term C_{norm} represents the normalized value of contribution of each of the vanadium ion species to the bulk transfer.

$$C_{\text{norm}} = \frac{z_2 D^m_2 \Delta c^m_2 + z_3 D^m_3 \Delta c^m_3 + z_4 D^m_4 \Delta c^m_4 + z_5 D^m_5 \Delta c^m_5}{z^2_2 D^m_2 c^m_2 + z^2_3 D^m_3 c^m_3 + z^2_4 D^m_4 c^m_4 + z^2_5 D^m_5 c^m_5} \tag{5}$$

Further, it is necessary to compute the ionic potential across the membrane. The ionic potential can be calculated by determining the voltage drop across the membrane. By using Ohm's law the membrane ionic potential can then be computed.

$$\varphi_m = i_{\text{tot}} * R_m \tag{6}$$

where 'i_{tot}' is the total current across the membrane which is the product of current density and the area of the membrane. R_m is the resistance of the membrane which causes the potential difference. The total membrane resistance can be obtained by integrating the resistivity along the thickness of the membrane 'd'.

$$R_m = \frac{1}{S_M}\int_0^d r_m(f)\,\mathrm{d}f \tag{7}$$

where $r_m(f)$ is the resistivity of the membrane along the axis of diffusion f. According to the reference [32], the local resistivity model for a Nafion type membrane is given by

$$r_m(f) = \frac{181.6\left[1 + 0.03J + \left(0.062\left(\frac{T_m}{303}\right)^2 J^{2.5}\right)\right]}{e^{\left(4.18\left(\frac{T_m - 303}{T_m}\right)\right)} \cdot [\lambda(f) - 0.634 - 3J]} \tag{8}$$

where J is the current density with cell current i_{tot} (A) and S_M is the membrane area in square meters.

$$J = \frac{i_{\text{tot}}}{10^4 (S_M)} \tag{9}$$

The description for all the variables mentioned in the above modeling equations is given in the nomenclature with the simulation parameters denoted in Table 1. The use of mathematical modeling along with chemistry to model a Redox Flow Battery to study the changes that happen in a battery due to change in external factors has proved to be very useful in monitoring the State of Charge (SOC) and capacity of the battery and to determine the battery charging/discharging processes to ensure maximum efficiency. A dynamic model is better suited to this particular need compared to a steady state model as it can monitor and act upon the transient changes in the characteristics of the battery in response to changes in operating conditions.

Dynamic models are developed on the basis of conservation of mass and energy to observe the changes in concentrations. A model dealing with the ion diffusion and side reactions for different membranes was developed by Tang et al. [7,26] who included the effect of temperature on the diffusion coefficients of the various species of vanadium ions for self-discharge reactions. A similar approach is used in the present model which has been extended to include the effect of bulk electrolyte transfer so as to provide a more accurate assessment of the state of the battery. Other assumptions made are:

- The charging/discharging current and the flow rate of the electrolyte are considered constant.
- The electrolytes are uniformly mixed and the chemical reactions due to diffusion are considered instantaneous.
- The ionic potential across the membrane is constant.
- Rates of charge/discharge reactions of the cell are described by Faraday's law of electrolysis.

Table 1
Parameters adopted in simulation [7,14,15].

Parameters	Value
Membrane surface area (S_M)	30 dm^2
Electrode surface area (S_E)	30 dm^2
Membrane thickness (d)	125×10^{-6} m
Upper voltage limit	1.7 V
Lower voltage limit	1.1 V
Upper concentration limit	1.99 mol L^{-1}
Lower concentration limit	0.01 mol L^{-1}
Current density (J)	60 mA cm^{-2}
Charging/Discharging current	180 A
Universal gas constant (R)	8.314 JK^{-1} mol^{-1}
Activation energy (E_a)	17341 J mol^{-1}
Formal potential (E_0)	1.4 V
Hydraulic permeability (k)	1.58×10^{-18}
Electro-kinetic permeability (k_φ)	1.13×10^{20}
Viscosity of bulk electrolyte (μ_w)	8.684×10^{-4} Pa s
Fixed acid concentration (c_f)	1990 mol m^{-3}
Initial volume (V)	Positive half-cell: 1 dm^3 Negative half-cell: 1 dm^3
Ionic potential of the membrane (φ_m)	660 mV

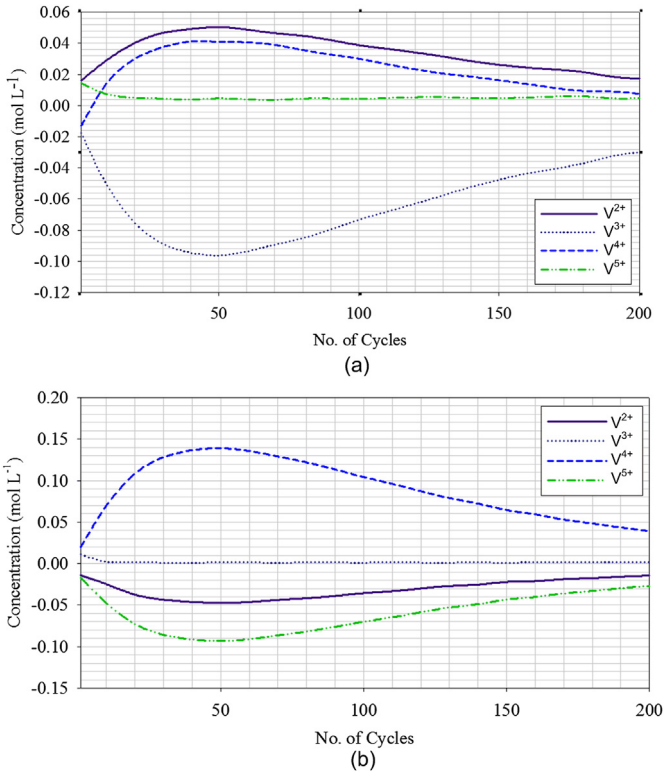

Fig. 2. Difference in diffusion trend due to temperature for Selemion CMV membrane (a) at 1.1 V (b) at 1.7 V.

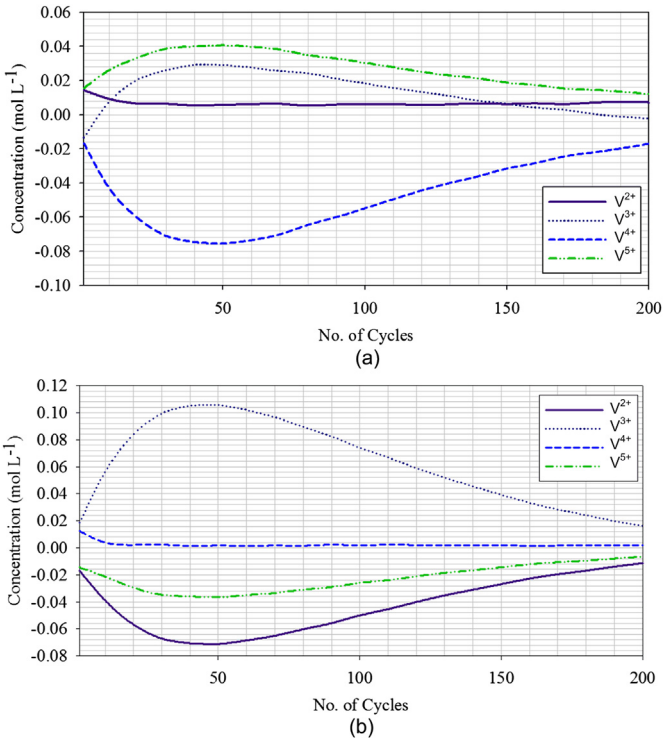

Fig. 3. Difference in diffusion trend due to temperature for Nafion 115 membrane (a) at 1.1 V (b) at 1.7 V.

The reactions between vanadium ions which occur in both the half cells influence the concentrations and need to be analyzed in the development of the model according to Tang et al. [26]:

$$V^{2+} + VO_2^+ \rightarrow 2VO^{2+} + e^-$$

$$V^{3+} + VO_2^+ \rightarrow 2VO^{2+}$$

$$VO_2^+ + V^{2+} + 4H^+ + e^- \rightarrow 2V^{3+} + 2H_2O$$

$$VO^{2+} + V^{2+} + 2H^+ \rightarrow 2V^{3+} + H_2O$$

The capacity of the battery is also affected by the side reactions of air oxidation of V(II) in the negative electrolyte and the evolution of hydrogen at the negative electrode during charging. These reactions can be overcome by employing an inert blanket or limiting the surface area to volume ratio thereby decreasing the reaction area in the case of air oxidation and by operating the battery in the range of 10–90% SOC to mitigate the problem of hydrogen evolution sacrificing some usable capacity [7,26]. In this paper, these side reactions are therefore ignored so as to focus on the effects of the diffusion processes on capacity decay.

The model used in this paper is developed by using the conservation of molar mass coupled together with the Arrhenius model for mass diffusivity. The diffusion of various species of vanadium ions across the membrane and the resulting chemical reactions mentioned above are taken into account. The diffusion coefficients employed for the model are calculated by taking into account the operational temperature of the battery. The dynamic concentrations thus calculated are then keyed into the Nernst equation to calculate the dynamic voltage of the cell during operation. This helps to establish the range of operating conditions and to determine the periods of charging and discharging to ensure optimal usage of the battery. The values chosen for the model are such that 200 charging cycles could be simulated for practical considerations of the parameters used. The dynamic equations based on the extended model for the process of charging and discharging is given by Eq. (10) as shown below:

$$\begin{aligned}
(V-\Delta V)\frac{dc_2}{dt} &= \pm\frac{JS_E}{zF} - D_2c_2\frac{S_M}{d}e^{-\frac{E_a}{RT}} - 2D_5c_5\frac{S_M}{d}e^{-\frac{E_a}{RT}} - D_4c_4\frac{S_M}{d}e^{-\frac{E_a}{RT}}\\
(V-\Delta V)\frac{dc_3}{dt} &= \pm\frac{JS_E}{zF} - D_3c_3\frac{S_M}{d}e^{-\frac{E_a}{RT}} + 3D_5c_5\frac{S_M}{d}e^{-\frac{E_a}{RT}} + 2D_4c_4\frac{S_M}{d}e^{-\frac{E_a}{RT}}\\
(V+\Delta V)\frac{dc_4}{dt} &= \pm\frac{JS_E}{zF} - D_4c_4\frac{S_M}{d}e^{-\frac{E_a}{RT}} + 3D_2c_2\frac{S_M}{d}e^{-\frac{E_a}{RT}} + 2D_3c_3\frac{S_M}{d}e^{-\frac{E_a}{RT}}\\
(V+\Delta V)\frac{dc_5}{dt} &= \pm\frac{JS_E}{zF} - D_5c_5\frac{S_M}{d}e^{-\frac{E_a}{RT}} - 2D_2c_2\frac{S_M}{d}e^{-\frac{E_a}{RT}} - D_3c_3\frac{S_M}{d}e^{-\frac{E_a}{RT}}
\end{aligned} \tag{10}$$

where c_2, c_3, c_4 and c_5 are the concentrations (mol L^{-1}) of V^{2+}, V^{3+}, V^{4+} and V^{5+} ions respectively. D_2, D_3, D_4 and D_5 are the maximum diffusion coefficients for V^{2+}, V^{3+}, V^{4+} and V^{5+} respectively whose values are calculated based on data in Refs. [26–28,33]. The signs of the dynamic equations are determined by whether the battery is being charged or discharged.

The state-space model for ion diffusion can be represented by:

$$\begin{aligned}
\dot{x} &= Ax + Bu\\
y &= Cx + Du
\end{aligned} \tag{11}$$

where the input vector is the current density "J" applied to the battery system and the state vector x is the concentration of different vanadium ion species.

$$x = [\,c_2 \quad c_3 \quad c_4 \quad c_5\,]^T$$

$$A = \begin{bmatrix} \frac{-D_2 S_M e^{\frac{-E_a}{RT}}}{d(V-\Delta V)} & 0 & \frac{-D_4 S_M e^{\frac{-E_a}{RT}}}{d(V-\Delta V)} & \frac{-2D_5 S_M e^{\frac{-E_a}{RT}}}{d(V-\Delta V)} \\ 0 & \frac{-D_3 S_M e^{\frac{-E_a}{RT}}}{d(V-\Delta V)} & \frac{2D_4 S_M e^{\frac{-E_a}{RT}}}{d(V-\Delta V)} & \frac{3D_5 S_M e^{\frac{-E_a}{RT}}}{d(V-\Delta V)} \\ \frac{3D_2 S_M e^{\frac{-E_a}{RT}}}{d(V+\Delta V)} & \frac{2D_3 S_M e^{\frac{-E_a}{RT}}}{d(V+\Delta V)} & \frac{-D_4 S_M e^{\frac{-E_a}{RT}}}{d(V+\Delta V)} & 0 \\ \frac{-2D_2 S_M e^{\frac{-E_a}{RT}}}{d(V+\Delta V)} & \frac{-D_3 S_M e^{\frac{-E_a}{RT}}}{d(V+\Delta V)} & 0 & \frac{-D_5 S_M e^{\frac{-E_a}{RT}}}{d(V+\Delta V)} \end{bmatrix}$$

The parameter B changes for charging and discharging processes as the reaction change leads to sign change for the different ion species in the equation.

$$B_{(Charging)} = \begin{bmatrix} \frac{S_E}{zF(V-\Delta V)} & 0 & 0 & 0 \\ \frac{-S_E}{zF(V-\Delta V)} & 0 & 0 & 0 \\ \frac{-S_E}{zF(V+\Delta V)} & 0 & 0 & 0 \\ \frac{S_E}{zF(V+\Delta V)} & 0 & 0 & 0 \end{bmatrix} \quad B_{(\text{Discharging})} = \begin{bmatrix} \frac{-S_E}{zF(V-\Delta V)} & 0 & 0 & 0 \\ \frac{S_E}{zF(V-\Delta V)} & 0 & 0 & 0 \\ \frac{S_E}{zF(V+\Delta V)} & 0 & 0 & 0 \\ \frac{-S_E}{zF(V+\Delta V)} & 0 & 0 & 0 \end{bmatrix}$$

$$C = \begin{bmatrix} 1 & 0 & 0 & 0 \\ 0 & 1 & 0 & 0 \\ 0 & 0 & 1 & 0 \\ 0 & 0 & 0 & 1 \end{bmatrix} \qquad D = 0$$

The modified cell voltage balance is derived from the Nernst equation and the cell resistance as given by Tang et al. Eq. (7). The cell voltage is calculated based on the open circuit voltage equation along with the cell resistance during charging and discharging processes. The proton concentration term in the Nernst Equation is combined with the standard potential term E_0 to produce formal potential E_0' which can be determined experimentally.

$$E(t) = E_0' + \frac{RT}{zF}\ln\left[\frac{c_2(t)\times c_5(t)}{c_3(t)\times c_4(t)}\right] \tag{12}$$

where E_0' is the formal cell potential measured at 50% state of charge. The formal cell potential for 2 M vanadium in 5 M sulfate electrolyte has been measured at 1.4 V [7].

4. Simulation results

Before moving on to discuss the results obtained during the simulation, it is important to define the parameters and the conditions under which the simulation is performed. For temperature dependence simulation, three different membranes (Selemion CMV, Selemion AMV and Nafion 115) are considered and the voltage limits for the battery are assumed to be 1.7 V as the upper limit and 1.1 V as the lower limit. The diffusion coefficients for each of the membrane is calculated separately by making use of the Arrhenius equation to calculate the respective activation energy and then reconstituting it to get the diffusion coefficient at a particular temperature. For the simulation of bulk electrolyte transfer across the membrane, the interval for iteration is taken as 1 cycle. Also the ionic potential across the membrane is calculated by using the voltage drop across the membrane from the electrical resistance of the Nafion 115 membrane obtained from Ref. [34] and from Eqs. (6)–(9).

The physical parameters for the simulation are set as given in Table 1. To avoid logarithmic zero term in Nernst equation, the initial values are taken as 1.99 mol L^{-1} for V^{5+} and V^{2+} and 0.01 mol L^{-1} for V^{3+} and V^{4+}. The initial simulation results are validated by comparing with the results from the Skyllas-Kazacos and Goh [23] and Tang et al. [7] models at 25 °C with the same parameters.

4.1. Results considering the effect of temperature

The concentration profiles for V^{2+}, V^{3+}, V^{4+} and V^{5+} are initially studied at 1.1 V and 1.7 V at different temperatures ranging from 10 °C to 40 °C. The trends in vanadium ion concentration with cycle number are consistent with those predicted in the diffusion model of Skyllas-Kazacos and Goh at room temperature for the Selemion CMV membrane [23]. To clearly illustrate the effect of temperature on the concentration of the vanadium ions, the concentration profiles for all the four ions are plotted by calculating the difference in diffusion between 10 °C and 40 °C at both ends of the charging/discharging cycles (1.1 V & 1.7 V) as shown in Fig. 2. The graph illustrates the trend of the difference in vanadium ion concentration change between the minimum and maximum temperatures (V^{x+} concentration trend at 40 °C − V^{x+} concentration trend at 10 °C).

The concentration trend difference between 40 °C and 10 °C is shown in the *Y* axis and the number of cycles is shown in the *X* axis in Fig. 3. Even though the characteristic curves of Nafion 115 membrane for temperature dependence looks similar to that of Selemion CMV on a superficial level, the extent of the diffusion of ion species is completely different.

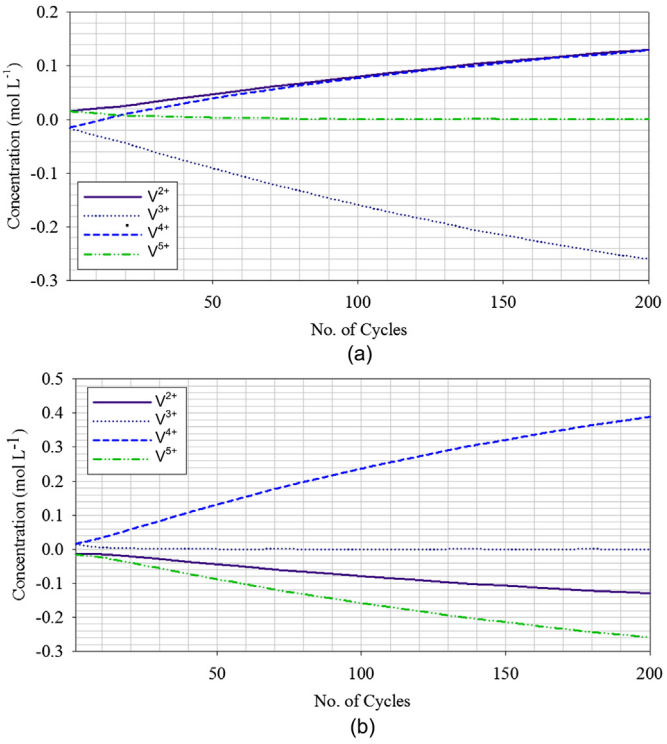

Fig. 4. Difference in diffusion trend due to temperature for Selemion AMV membrane (a) at 1.1 V (b) at 1.7 V.

The concentration profiles for all the four ions at 40 °C with respect to 10 °C over 200 cycles at both ends of the charging/discharging cycle (1.1 V & 1.7 V) is plotted. As shown in Fig. 4 for Selemion AMV membrane based cells, the difference in diffusion however does not reduce as the cycling progresses after 50 cycles. Instead the difference keeps on increasing as the number of battery charging/discharging cycles increases. It is observed that the relative difference also varies linearly with the number of cycles and does not equalize as the difference keeps on increasing as the number of battery charging/discharging cycles increase. This is in contrast to the behavior of vanadium ions across the Selemion CMV and Nafion 115 membranes.

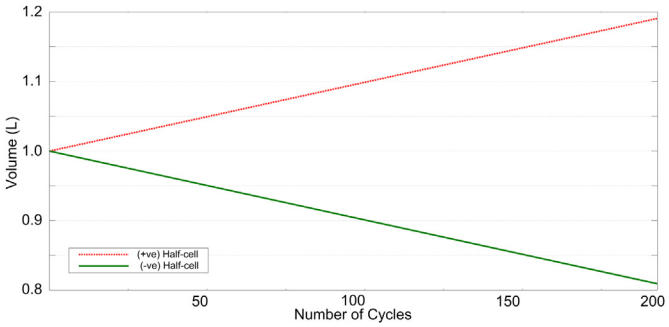

Fig. 6. Change in volume due to bulk electrolyte transfer for 200 cycles.

4.2. Results including bulk electrolyte transfer across the membrane

The bulk electrolyte transfer across the membrane is caused mainly by: 1) the osmosis phenomena, 2) the drag of water molecules induced by the diffusion of the vanadium ion species across the membrane and 3) the transfer of water with the protons as they move through the membrane to balance the charge. The number of water molecules transferred by the protons will vary for different membranes. Considering the practical applicability, the analysis for the bulk electrolyte transfer phenomena is done for Nafion 115 membrane including all the factors influencing volume change as discussed above.

The osmotic pressure change between the two half cells for 200 cycles for 4 different temperatures with the pressure value in Pascal on the *Y* axis and number of cycles in the *X* axis is shown in

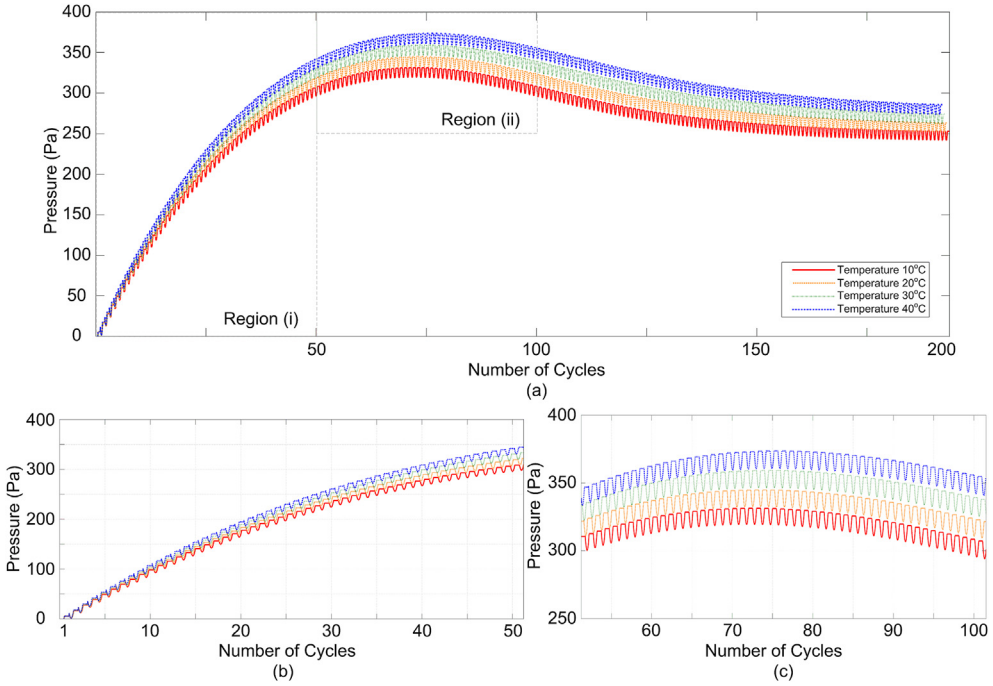

Fig. 5. a) Change in Osmotic pressure as a function of ionic concentration, b) Region 1 (0–50 cycles), c) Region 2 (50–100 cycles).

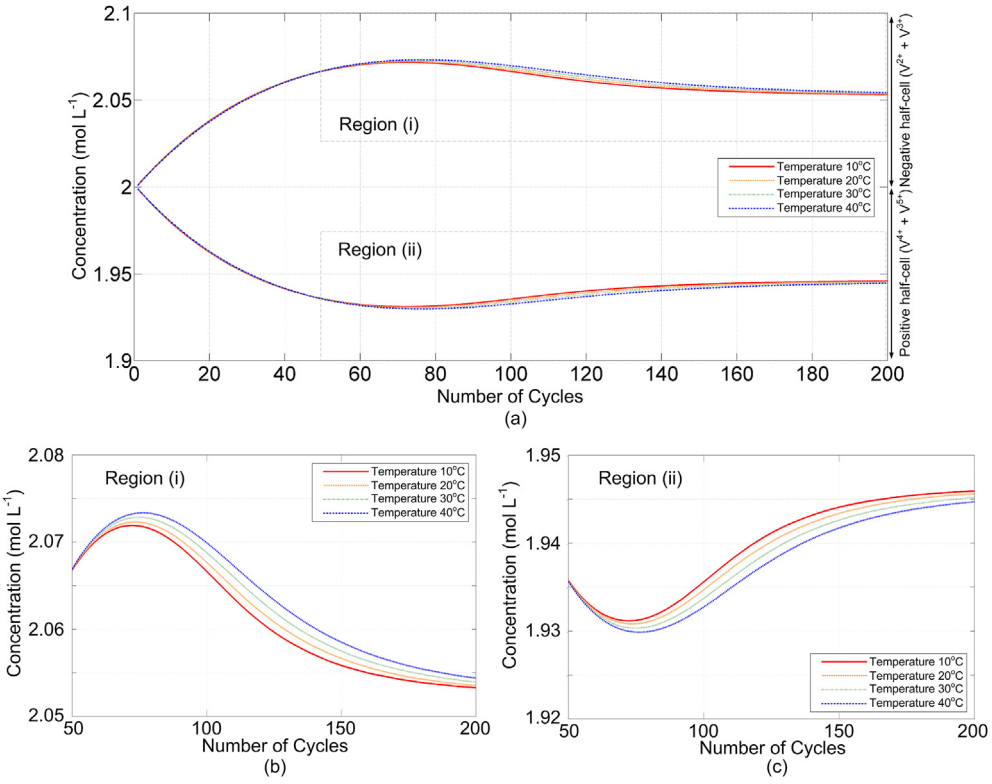

Fig. 7. a) Change in half-cell concentration at different temperatures, b) Region 1 – Negative half-cell (50–200 cycles), c) Region 2 – Positive half-cell (50–200 cycles).

Fig. 5. The osmotic pressure change is given as a function of the ionic concentration of the vanadium ion species in the half-cells. From the figure, it can be observed that the increase in pressure is significantly steep for the first 50 cycles and tends to stabilize around the 50–100 cycles range with maxima at 75th cycle.

The change of volume in each of the two half cells for 200 cycles with the volume change in Liters given on the *Y* axis and number of cycles in the *X* axis is shown in Fig. 6. From the figure it can be observed that there is about 19% change in volume in each of the half-cell where the electrolyte from the negative half-cell is transferred to the positive half-cell which is in conformity with the work by Sukkar et al. [35] for a cation type ion exchange membrane. The total volume of the battery however remains constant following the law of conservation of mass. This change in volume has immediate effect on the diffusion behavior of the vanadium ions and the overall concentration change in the cell. The total concentration change in each of the half-cell is plotted in Fig. 7 where the positive half-cell concentration constitutes of the concentration if V^{4+} and V^{5+} ions. The negative half-cell concentration constitute of the concentrations of V^{2+} and V^{3+} ions which is plotted in the same figure. As it can be observed, the concentration in the negative half-cell increases initially and stabilizes after decreasing with maxima at the 75th cycle. The concentration is plotted for 4 different temperatures with the region of 50–200 cycles emphasized in the figure for better understanding.

The change in volume has a direct effect in the diffusion characteristics of each species of vanadium ions present in the battery. The change in the concentration of V^{2+} ions at different temperatures is shown in Fig. 8. The characteristics of V^{2+} at 1.7 V are shown with ion concentration on the *Y* axis and the number of cycles on the *X* axis. At 1.1 V, the concentration decreases to zero mol L^{-1} soon after the cycling starts and hence it is not shown in the figure. At 1.7 V, the concentration remains in the initial state until the volume change dominates causing it to increase and stabilize with a change of 5% to the initial concentration which is shown in Fig. 8.

The plots showing the trend of concentration of vanadium ions are all plotted along the same *Y* axis parameter of concentration in mol L^{-1} and the *X* axis parameter of number of cycles till 200 cycles. The concentration change for V^{3+} ion at 1.1 V and 1.7 V for temperatures ranging from 10 °C to 40 °C is shown in Fig. 9. The concentration profile of V^{3+} at the end of charge suffers a slight bulge during the initial cycling; however, the effect of volume change makes the concentration stabilize at the end of 200 cycles. At the end of discharging; the concentration increases and reaches steady state. There is a decrease in the concentration after 75th cycle with a very small slope before reaching the steady state. The concentrations of V^{3+} and V^{2+} ions complement each other and contribute to the overall balance in the negative half-cell.

The concentration change of V^{4+} ions at the end of discharge and charge cycles respectively is shown in Fig. 10. The change that is observed is only about 20% in the case of 1.1 V shown in Fig. 10a

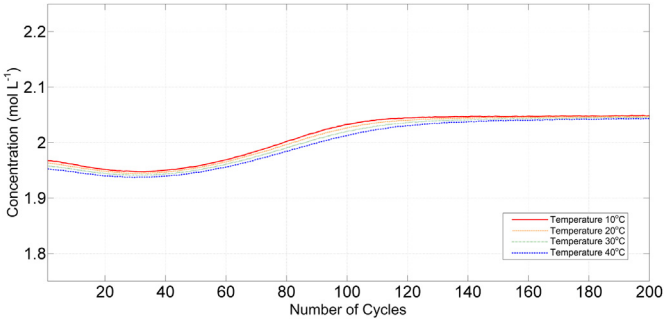

Fig. 8. Concentration change for V^{2+} ions for 200 cycles at 1.7 V.

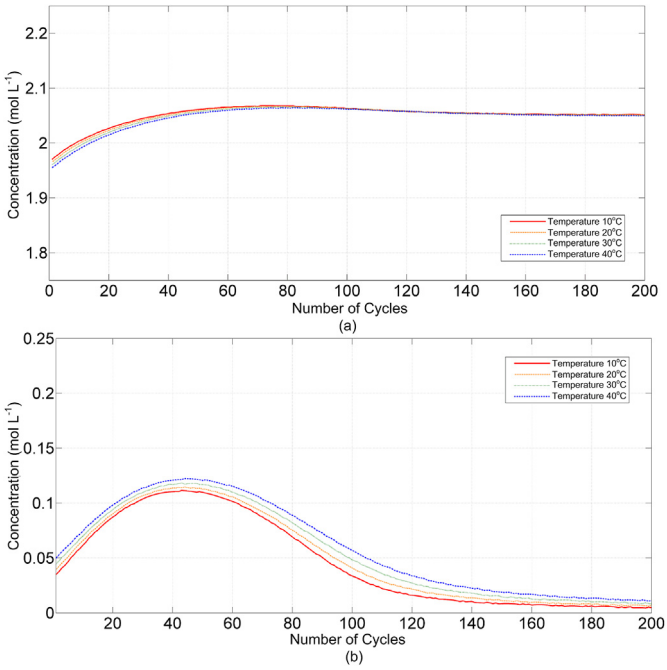

Fig. 9. Concentration change for V^{3+} ions for 200 cycles (a) At 1.1 V, (b) At 1.7 V.

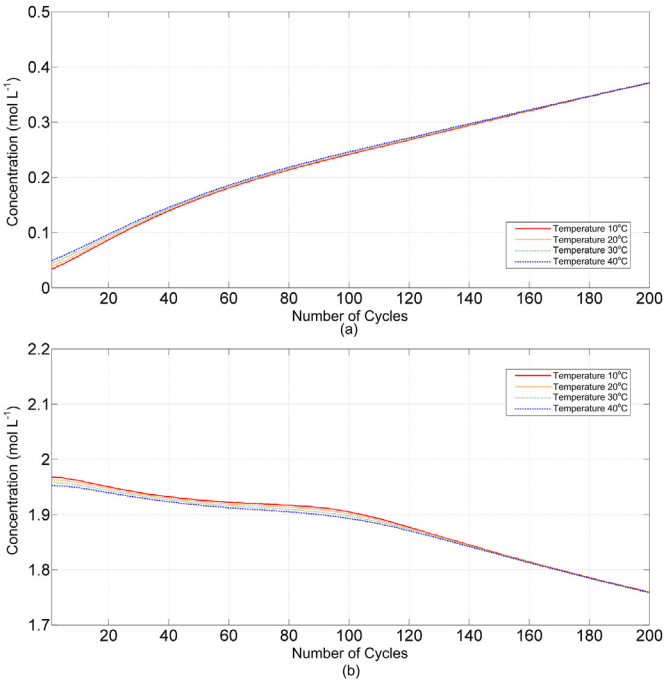

Fig. 11. Concentration change for V^{5+} ions for 200 cycles (a) At 1.1 V, (b) At 1.7 V.

where there is a steep decrease of V^{4+} concentration to 1.575 mol L^{-1} at the end of cycling. The change at 1.7 V is observed only latter half of operation and the trend takes a positive slope to reach 0.18 mol L^{-1}. It can also be inferred that when the cycling proceeds towards the end, the effect of temperature on the ion diffusion decreases and is almost nil at the end of the respective charge and discharge cycles.

Similar to the complementary relationship between V^{2+} and V^{3+}, V^{5+} ions complement for V^{4+} ions thereby contributing to the overall concentration in the positive half-cell. The concentration of V^{5+} ions at 1.1 V increases with a steady positive slope and deviates to 15.7% from the initial value. The concentration at the end of charge cycle decreases from the initial value to about 9.5% at the end of 200 cycles. The rate of decrease is not constant throughout the period as the slope increases post first 100 cycles as shown in Fig. 11b.

The capacity of the battery is plotted in Fig. 12 for different temperatures, including the phenomenon of bulk electrolyte transfer. The capacity in ampere hours is given on the *Y* axis, against the number of cycles in the *X* axis. Considering the change in the volume of the half-cells during the cycling process and the effect it has on the concentration of the vanadium ions, the capacity curve also follows a trend in accordance. Initially, the capacity decreases and as expected, it tends to reach a steady state around 100 cycles. The capacity decay slope is high in the last 100 cycles of operation as it follows the concentration trend of the vanadium ions in the half-cells. The effect of temperature on the overall capacity change is very small as the cycling progresses and becomes negligible at the end of 200th cycle with not a very significant effect during the process of cycling as that of the bulk electrolyte transfer.

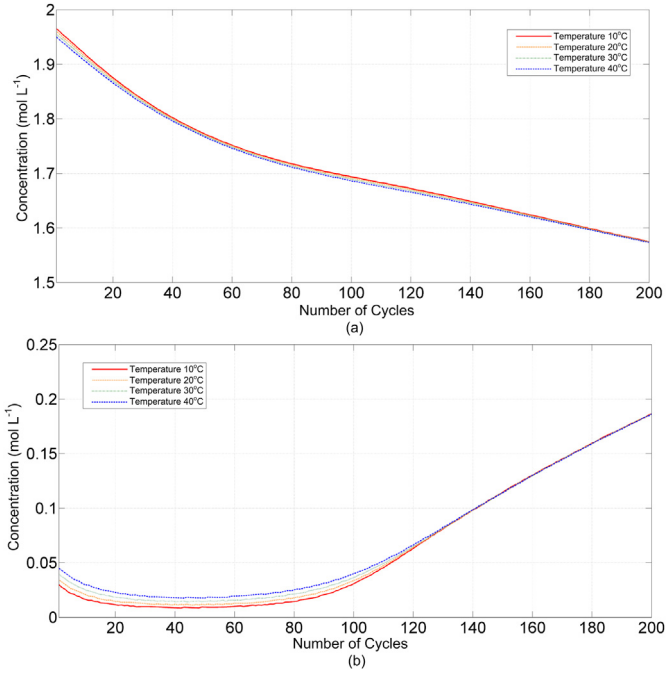

Fig. 10. Concentration change for V^{4+} ions for 200 cycles (a) At 1.1 V, (b) At 1.7 V.

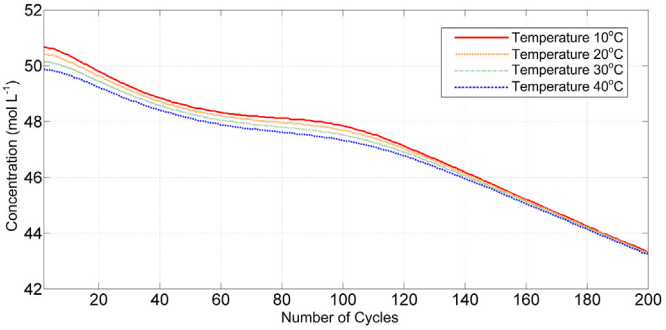

Fig. 12. Capacity decay in Nafion 115 membrane at different temperatures.

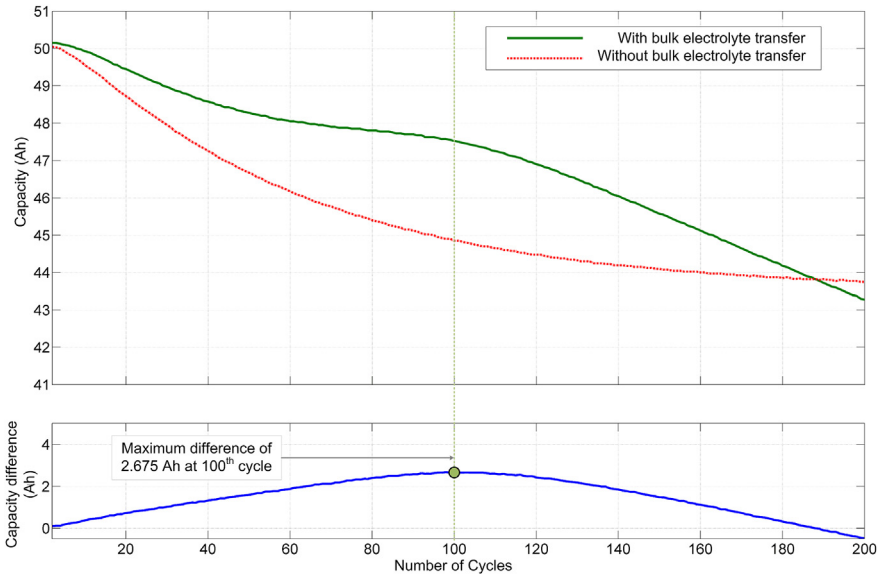

Fig. 13. Comparison of capacity change with and without bulk electrolyte transfer phenomenon across 200 cycles at 30 °C.

On comparing the effect of bulk electrolyte transfer on capacity decay due to ion diffusion, it can be observed from Fig. 13 that there is no big difference at the end values of both simulations. There is a very significant difference however, in the trend followed to reach the final value. With the consideration of bulk electrolyte transfer phenomena, there are 2 stages of decay trend with different slopes as shown. On computing the maximum difference between both the trends, it is observed at the 100th cycle with a difference of 2.675 Ah. Further, to observe the decay in the capacity due to the effect of temperature is done by comparing the width of the voltage curves at different temperatures. The voltage curves of the battery at different temperatures around the 50th cycle of operation is shown in Fig. 14. It can be observed that the plot corresponding to 40 °C is lagging the 10 °C plot due to the cumulative decrease in the capacity due to temperature causing decrease in the width of the voltage curve.

5. Discussion

One of the main reasons for capacity decay in VRB is due to interaction of Vanadium ions that diffuse from one half-cell to another half-cell. The diffusion of ions across the ion exchange membrane varies significantly from one membrane to another and is influenced by many factors ranging from charging current to temperature. The temperature effect on diffusion and hence the capacity decay is analyzed in this paper. In this paper the temperature is considered to remain constant for the whole period of operation. In reality however, the temperature of the stack increases with the cycle number. This variation is not taken into account for this model as it would complicate the dynamic equations and has a very little effect in the overall capacity loss. Further, the diffusion coefficients considered for the simulations are theoretically calculated based on literature and may not be very accurate. Actual diffusion coefficients can be calculated by experimentation and added to study the temperature effect on the different membranes more precisely.

The effect of temperature on capacity decay is studied for three different membranes namely, Selemion CMV, Nafion 115 and Selemion AMV. It is observed that the effects of temperature for the Selemion CMV and Nafion 115 membranes are confined to the initial 25–100 battery discharging/charging cycles and that the characteristics equalize as the number of cycles increase. Also, the maximum difference for concentration of Vanadium ions between the 10° Celsius and 40 °C is seen to be around 50 cycles for both Selemion CMV and Nafion 115. As for the capacity, it follows a trend similar to that of the concentration and as the maximum difference at around 50 cycles and tends to equalize as the number of cycles increase. The intrinsic loss due to the temperature difference however results in a loss of overall capacity in the batteries. The results for Selemion AMV are very different from that of Selemion

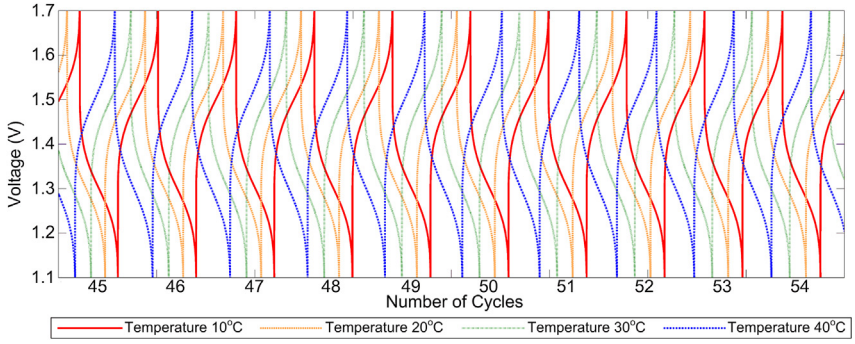

Fig. 14. Voltage plot at different temperatures.

CMV and Nafion 115. In the case of Selemion CMV and Nafion 115 membranes, the order of diffusion coefficient values is $V^{2+} > V^{4+} > V^{5+} > V^{3+}$. From the self-discharge reaction however it can be observed that for a given amount of V^{2+} ions passing through the membrane more V^{5+} ions are consumed to form V^{4+} ions and these changes slow down as the number of ions to cause the reaction decreases leading to a stabilization around 200 cycles. Unlike cation type membrane, the Selemion AMV membrane repels the vanadium cations which accounts for the lower value of diffusion coefficients of the membrane. The lower diffusion coefficients does not necessarily warrant a better performance of the battery as the differential transfer of the vanadium ions across the membrane produces an imbalance causing more and more ions to diffuse through the membrane. The change in concentration seems to be linear with respect to the number of charging/discharging cycles and the gradient for change in concentration for both positive and negative gradients increase with the increase in temperature. As a result the difference in concentration of Vanadium ions between that of 40 °C and that of 10 °C increase as the number of cycles increase and do not equalize at the end. Further, as the capacity decreases, the time for charging and discharging the battery also reduces eventually.

It is observed that bulk electrolyte transfer across the membrane has a significant effect on the concentration change over 200 cycles and eventually the battery capacity. This is modeled for the Nafion 115 membrane that has been widely studied for the VRB, although not used commercially. The extended model developed for simulation includes the effect of temperature and the bulk electrolyte transfer phenomena to study the characteristics of ion diffusion. For reducing computational complexity, the ionic potential across membrane is assumed as constant throughout the whole period while calculating the velocity across the membrane. The change in volume between the half-cells may not be linear in practical case, considering all the other environmental parameters affecting the bulk electrolyte movement across the membrane, including hydraulic pressure differences from pump operation. On comparing the results with the models neglecting the effect of bulk electrolyte transfer, a substantial difference in the ion diffusion behavior of the different vanadium ions can be observed making the proposed model more comprehensive.

6. Conclusion

An extended dynamic model is developed to predict the capacity of the battery with the concentration obtained from initial simulations. The predicted capacity is then used to identify the capacity loss due to the cross-contamination process over long periods of operation at different temperatures. The temperature effect on the change in concentration of Vanadium ions is investigated for three different membranes namely Selemion CMV, Nafion 115 and Selemion AMV for temperatures ranging from 10 °C to 40 °C. It is seen that the loss in capacity of the battery increases with the increase in temperature and the decay behavior is dependent on the membrane type. The two cation exchange membranes, Selemion CMV and Nafion 115 experienced the maximum amount of capacity loss during the first 100 operating cycles and seemed to stabilize as the number of cycles increased. For the anion exchange Selemion AMV membrane however, the capacity loss seemed to increase linearly as the number of cycles increased and showed no sign of stabilizing. The dominant part of the capacity loss (change in capacity) due to the temperature change stems from the different values for diffusion coefficients of each species of Vanadium ions which are also temperature dependent as shown in the paper. Nafion 115 membrane is considered for studying the combined effect of bulk electrolyte transfer and temperature in capacity fade. There is a 19% change in volume due to the bulk electrolyte transfer phenomena with a 0.5% tolerance for the temperature change. This translates to a considerable change in the concentration trend across 200 cycles from the initial concentration. The overall concentration in each half-cell tends to stabilize after 75 cycles of operation. The capacity characteristics can be analyzed in two regions, region 1 from 1 to 100 cycles and region 2 from 100 to 200 cycles. The average slope showing the rate of capacity decay in region 1 is 5.2% and the average slope for capacity decay in region 2 is 8.9%. The overall capacity decay due to diffusion for Nafion 115 membrane is 13.8% with 2% tolerance for the temperature difference.

Acknowledgment

This research is funded by the Republic of Singapore's National Research Foundation through a grant to the Berkeley Education Alliance for Research in Singapore (BEARS) for the Singapore–Berkeley Building Efficiency and Sustainability in the Tropics (SinBerBEST) Program. BEARS has been established by the University of California, Berkeley as a center for intellectual excellence in research and education in Singapore.

References

[1] M. Skyllas-Kazacos, M. Chakrabarti, S. Hajimolana, F. Mjalli, M. Saleem, J. Electrochem. Soc. 158 (2011) R55–R79.
[2] A.Z. Weber, M.M. Mench, J.P. Meyers, P.N. Ross, J.T. Gostick, Q. Liu, J. Appl. Electrochem. 41 (2011) 1137–1164.
[3] M. Rychcik, M. Skyllas-Kazacos, J. Power Sources 22 (1988) 59–67.
[4] A. Shibata, K. Sato, Power Eng. J. 13 (1999) 130–135.
[5] P. Zhao, H. Zhang, H. Zhou, J. Chen, S. Gao, B. Yi, J. Power Sources 162 (2006) 1416–1420.
[6] E. Sum, M. Rychcik, M. Skyllas-Kazacos, J. Power Sources 16 (1985) 85–95.
[7] A. Tang, J. Bao, M. Skyllas-Kazacos, J. Power Sources 196 (2011) 10737–10747.
[8] C.J. Rydh, J. Power Sources 80 (1999) 21–29.
[9] H. Prifti, A. Parasuraman, S. Winardi, T.M. Lim, M. Skyllas-Kazacos, Membranes 2 (2012) 275–306.
[10] D. Chen, S. Kim, V. Sprenkle, M.A. Hickner, J. Power Sources 231 (2013) 301–306.
[11] C. Jia, J. Liu, C. Yan, J. Power Sources 195 (2010) 4380–4383.
[12] C. Jia, J. Liu, C. Yan, J. Power Sources 203 (2012) 190–194.
[13] Q. Luo, L. Li, Z. Nie, W. Wang, X. Wei, B. Li, B. Chen, Z. Yang, J. Power Sources 218 (2012) 15–20.
[14] S. Corcuera, M. Skyllas-Kazacos, Eur. Chem. Bull. 1 (2012) 511–519.
[15] E. Agar, A. Benjamin, C. Dennison, D. Chen, M. Hickner, E. Kumbur, J. Power Sources 246 (2014) 767–774.
[16] A.H. Whitehead, M. Harrer, J. Power Sources 230 (2012) 271–276.
[17] T. Mohammadi, M.S. Kazacos, J. Power Sources 63 (1996) 179–186.
[18] Xiong Binyu, Jiyun Zhao, Zhongbao Wei, Maria Skyllas-Kazacos, J. Power Sources 262 (2014) 50–61.
[19] D. You, H. Zhang, C. Sun, X. Ma, J. Power Sources 196 (2011) 1578–1585.
[20] B. Ge, W. Wang, D. Bi, C.B. Rogers, F.Z. Peng, A.T. de Almeida, H. Abu-Rub, Int. J. Electr. Power & Energy Syst. 44 (2013) 115–122.
[21] M. Vynnycky, Energy 36 (2011) 2242–2256.
[22] A. Shah, M. Watt-Smith, F. Walsh, Electrochim. Acta 53 (2008) 8087–8100.
[23] M. Skyllas-Kazacos, L. Goh, J. Memb. Sci. 399 (2012) 43–48.
[24] M. Vijayakumar, L. Li, G. Graff, J. Liu, H. Zhang, Z. Yang, J.Z. Hu, J. Power Sources 196 (2011) 3669–3672.
[25] M. Vijayakumar, W. Wang, Z. Nie, V. Sprenkle, J. Hu, J. Power Sources 241 (2013) 173–177.
[26] A. Tang, J. Bao, M. Skyllas-Kazacos, J. Power Sources 216 (2012) 489–501.
[27] Z. Wei, J. Zhao, M. Skyllas-Kazacos, B. Xiong, J. Power Sources 260 (2014) 89–99.
[28] B. Xiong, J. Zhao, K. Tseng, M. Skyllas-Kazacos, T.M. Lim, Y. Zhang, J. Power Sources 242 (2013) 314–324.
[29] E. Agar, K. Knehr, D. Chen, M. Hickner, E. Kumbur, Electrochim. Acta 98 (2013) 66–74.
[30] K. Knehr, E. Agar, C. Dennison, A. Kalidindi, E. Kumbur, J. Electrochem. Soc. 159 (2012) A1446–A1459.
[31] H. Al-Fetlawi, A. Shah, F. Walsh, Electrochim. Acta 55 (2009) 78–89.
[32] F.B. Gao, Benjamin, Abdellatif Miraoui, Proton Exchange Membrane Fuel Cell Modeling, ISTE Ltd; John Wiley & Sons, Inc, 2012.
[33] C. Sun, J. Chen, H. Zhang, X. Han, Q. Luo, J. Power Sources 195 (2010) 890–897.
[34] C.R.-P. Moises Bautista-Rodriguez, Araceli, Atonio J. Rivera-Marquez, Omar Solorza-Feria, Int. J. Electrochem. Sci. (2009) 43–59.
[35] T. Sukkar, M. Skyllas-Kazacos, J. Memb. Sci. 222 (2003) 235–247.